Biochemical and Biophysical Research Communications **267,** 17–21 (2000)
doi:10.1006/bbrc.1999.1907, available online at http://www.idealibrary.com on IDEAL®

Purification and Characterization of Perlucin and Perlustrin, Two New Proteins from the Shell of the Mollusc *Haliotis laevigata*

Ingrid M. Weiss,* Stefan Kaufmann,† Karlheinz Mann,‡ and Monika Fritz*,[1]

**Institut für Biophysik, Physik Department der TU-München, E22, James-Franck-Strasse, 85747 Garching, Germany; †Nimbus GmbH, Karl-Heine Strasse 99, 04229 Leipzig, Germany; and ‡Max-Planck-Institut für Biochemie, Am Klopferspitz 18a, 82152 Martinsried, Germany*

Received November 15, 1999

Two new proteins, named perlucin and perlustrin, with M_r 17,000 and 13,000, respectively, were isolated from the shell of the mollusc *Halotis laevigata* (abalone) by ion-exchange chromatography and reversed-phase HPLC after demineralization of the shell in 10% acetic acid. The sequence of the first 32 amino acids of perlucin indicated that this protein belonged to a heterogeneous group of proteins consisting of a single C-type lectin domain. Perlucin increased the precipitation of $CaCO_3$ from a saturated solution, indicating that it may promote the nucleation and/or the growth of $CaCO_3$ crystals. With pancreatic stone protein (lithostathine) and the eggshell protein ovocleidin 17, this is the third C-type lectin domain protein isolated from $CaCO_3$ biominerals. This indicates that this type of protein performs an important but at present unrecognized function in biomineralization. Perlustrin was a minor component of the protein mixture and the sequence of the first 33 amino acids indicated a certain similarity to part of the much larger nacre protein lustrin A.

Key Words: **perlucin; perlustrin; abalone; mollusc shell; organic matrix; C-type lectin domain; nucleation.**

The abalone shell is a remarkable biogenic composite material and has attracted much attention in material science because of its unusual properties (1, 2). While the outer layer of the shell (the prismatic layer) consists of the calcitic polymorph of calcium carbonate, the inner layer (nacre or mother of pearl) is formed from aragonite tablets or lamellae with a diameter of about 15 μm and a height of about 0.5 μm (3). The aragonite tablets are uneven hexagons which are embedded in an organic matrix (4, 5). The organic matrix consists of interlamellar sheets, connecting elements between the interlamellar sheets and intracrystalline proteins (6). The interlamellar sheets are multilamellar and have a core of insoluble material, predominantly chitin, embedded in tightly connected, insoluble protein layers (7). The organic matrix of nacre, which is only 1–5% by weight, is thought to nucleate and direct the growth of the mineral component and to act as a glue preventing crack protrusion through the shell. The fracture toughness of nacre is about three orders of magnitude higher than that of pure aragonite (8).

The abalone shell is formed during the transformation of larvae to the juvenile animal (9). The calcium carbonate deposited first is the calcite polymorph, then aragonite layers are built up on top of it. The proteins accompanying the formation of mineral phases are different in the different layers (6). *In vitro,* solutions of these proteins control aragonite or calcite polymorphism (10, 11) and modify the growth of geologic calcite crystals (12). Most of the proteins known at present are rich in aspartic acid and bind calcium (13). We report for the first time the purification of a C-type lectin domain protein from nacre. First, *in vitro* experiments on the function of this protein (perlucin) showed that it increases $CaCO_3$ precipitation and promotes the formation of crystals on hydrophobic surfaces. In addition a minor component, perlustrin, was isolated and identified as a new protein with a certain similarity of its N-terminal sequence to part of the sequence of lustrin A (14).

MATERIALS AND METHODS

Collection of the crude protein material. Shells of the species *Haliotis laevigata* were obtained from the Australian Abalone Exports PTY.LTD. (Victoria, Australia). For preparation of nacre (mother of pearl) the shells were sand blasted to completely remove the calcitic part. The aragonitic fraction was rinsed with 25 mM Tris buffer, pH 7.4, cracked in a bench vice and placed into a dialysis tubing (Visking Typ 8/32 cutoff 15 kDa, Roth, Karlsruhe) filled with the same buffer. One end of the tubing was not closed but connected to a tube for collection of the overflow. The following steps were carried out at 4°C. By addition of 10% acetic acid (2.5 ml/g), the solution began to develop foam due to the release of carbon dioxide.

[1] To whom correspondence should be addressed. Fax: ++49 (0)89 2891 2469. E-mail: mfritz@physik.tu-muenchen.de.

0006-291X/00 $35.00

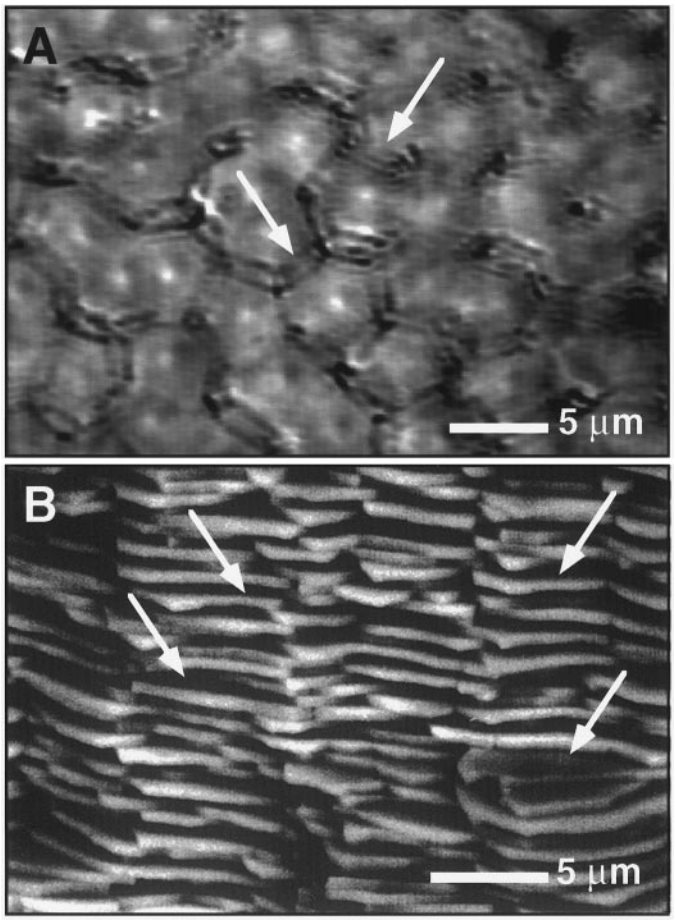

FIG. 1. Images of different parts of nacre in light microscopy and scanning electron microscopy (SEM). (A) Light microscopic image of the organic components of nacre. The honeycomb-like structure consists of horizontal protein layers with a core of chitin and vertical "walls" (arrows) between the horizontal layers. (B) SEM image of mature abalone nacre. The tablets (white arrows) consist of the mineral aragonite ($CaCO_3$). Their diameter is 10 to 15 μm and their height is about 500 nm. They are well-ordered in horizontal, confluent layers where each of the tablet shows an uneven hexagon. An uninterupted nacrous layer can be thousands of layers thick.

The overflow of the foaming solution was collected until foaming stopped. By changing the dialysis buffer against fresh 10% acetic acid, the foaming started again and the overflow was collected in a second tube. In this way six fractions of 4–40 ml of foam raw extract were obtained in one week. The foam fractions and the remaining suspension were centrifuged at 5445*g* for 50 min at 4°C. The supernatants were dialyzed against three changes of 30 volumes of 25 mM Tris, pH 7.4, 0.002% NaN_3, sterilized by filtration through a filter with pores of 0.22 μm and stored at 4°C.

Purification of perlucin and perlustrin. Ion exchange chromatography was done using a Pharmacia CM-Sepharose Fast Flow HiTrap column with a linear gradient of 0–1 M NaCl in 25 mM citrate buffer, pH 5.0, in 20 min at a flow rate of 1 ml/min. Protein fractions were concentrated in a speed vac concentrator and analyzed by SDS-PAGE using a 10–20% gradient BioRad Ready-Gel system. For final purification the fractions obtained by ion exchange chromatography were acidified to pH ~1 with trifluoroacetic acid and subjected to reversed phase HPLC on a C4 column (Vydac 214TP5405, 50 × 4.6 mm) using a gradient of 7–70% acetonitrile in 0.1% trifluoroacetic acid at a flow rate of 0.5 ml/min for 55 min. N-terminal amino acid sequence analysis was done using a PE-Applied Biosystems sequencer Model 473A after desalting of the samples with the ProSorb device (PE-Applied Biosystems) or after reversed phase HPLC. Pyridylethylation followed established protocols. Database searches were done using the FASTA program of the GCG Program Package, version 9 (Genetics Computer Group, Madison, WI).

Saturated calcium carbonate solution. 3 ml of 20 mM $CaCl_2$ (in 3 mM Tris, pH 8.7) was poured into 3 ml of 20 mM $NaHCO_3$ (in 3 mM Tris, pH 8.7) at t = 0 to create the saturated $CaCO_3$ solution. Perlucin (30 μg) was introduced in 50 μl of 3 mM Tris, pH 8.7 to the solution at t = 0. The control measurements were done by adding 50 μl 3 mM Tris, pH 8.7. There was a sudden downward shift in the pH when we poured the $CaCl_2$ into the hydrogen carbonate solution. This shift is well known, not understood, but very reproducible and is recorded to determine calcium carbonate precipitation (15).

Crystallization studies with perlucin in saturated calcium carbonate solution. For saturated $CaCO_3$ solution we followed the protocol of Hillner *et al.* (16). 30 to 50 ml of 100 mM $NaHCO_3$ were added dropwise to 120 ml of 40 mM $CaCl_2$ while stirring until the solution became turbid. Then the pH was adjusted to 8.2 with 1 M NaOH. The solution was centrifuged and filtered sterile (0.22 μm). 50 μl of 0.1 mg/ml perlucin in Tris, pH 8.2, was added to 150 μl of the saturated solution. As a control buffer solution without protein was used. Each of the solutions was incubated at 4°C for one week in a Teflon trough (hydrophobic surface) containing a hydrophilic cover glass.

RESULTS AND DISCUSSION

The Microscopic Structure of Nacre

Nacre is a highly organized composite material where aragonite tablets are embedded in a mold of

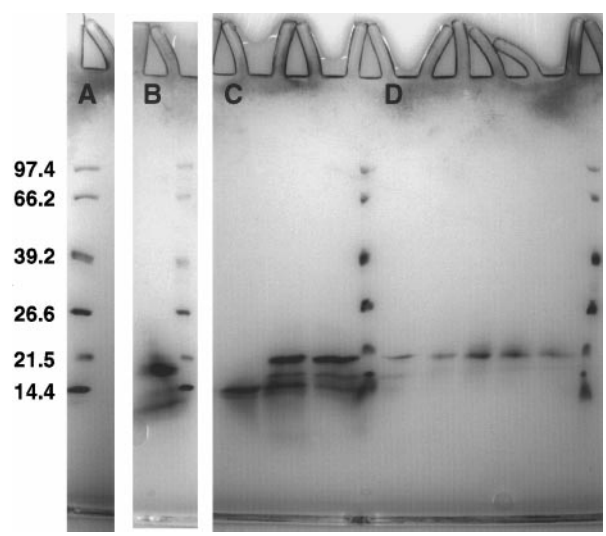

FIG. 2. SDS-PAGE of the ion-exchange chromatography purification steps. PAGE was done with 10–20% acrylamide gradient gels. (A) Molecular weight standards with masses in kDa indicated on the left. (B) Protein band pattern of foam fractions. The pattern of bands in the residual suspension was almost identical. The aragonitic phase of the shell contained three proteins with 17, 15, and 13 kDa. (C) A 13 kDa protein which did not yield an N-terminal amino acid sequence was eluted first during the purification with ion-exchange chromatography. It is not clear at present whether this protein is identical with perlustrin. (D) Second elution peak which contained almost pure perlucin (17 kDa).

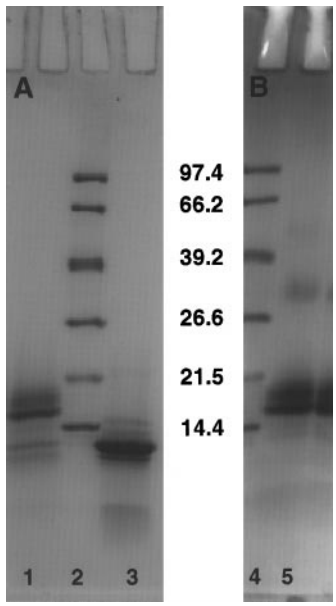

FIG. 3. PAGE of the purified proteins perlustrin and perlucin after reversed phase chromatography. (A) Lane 1, the protein band pattern of the protein solution from the second elution peak in Fig. 2D after separation by ion exchange chromatography. Lane 2, molecular weight standards with masses in kDa indicated on the right. Lane 3, purified perlustrin with a molecular weight of about 13 kDa. (B) Lane 4, molecular weight standards with masses in kDa indicated on the left. Lane 5, perlucin eluted in two peaks of unequal size. The proteins in both peaks showed the same N-terminal sequence.

organic matrix (3, 17). The organic matrix forms thin sheets of about 50 nm between the aragonite tablets. After demineralization of nacre with 10% acetic acid the organic mold can be made visible. In phase contrast light microscopy honey comb like structures of organic material appear (Fig. 1A). This structure is composed of a vertical layer of chitin (data not shown), an attached layer of proteins and connecting bridges between the layers. Both of the latter can be degraded by proteinase K (7). The aragonite tablets with a size of about 10 $\times$ 0.5 μm (Fig. 1B, white arrows) form confluent layers inbetween the organic mold. Several vertical consecutive tablets are single crystals with the inherent matching of crystal vectors. As there are organic sheets between these vertical consecutive tablets the question rises whether the organic sheets act as templates for the next mineral layer or whether there is another mechanism responsible for this, like mineral bridges between the aragonite layers (7). In any case the organic material is an important factor in nacre and characterization of the proteins involved and functional studies will be necessary to understand the formation of this composite material.

Isolation of Proteins

Fresh, whole shells of *Haliotis laevigata* (abalone) were used to collect the crude protein material. After removing the calcitic part of the shells by sand blasting the remaining nacre was crunched to small pieces of a few centimeter in diameter and placed into dialysis tubing open at one side and filled with 25 mM Tris buffer, pH 7.4. After adding acidic acid to the exchange buffer the shell pieces started to demineralize and a foam was formed due to CO_2 formation. SDS-PAGE of foam fractions and the remaining suspension after removal of insoluble material showed essentially the same protein pattern consisting of two major and one minor protein bands (Fig. 2). The major proteins had an M_r of about 17,000 and about 13,000 and the minor protein had an M_r of about 15,000. The 15 kDa protein might be the intracrystalline protein which is incorporated into single tablets of nacre (11). A 17 kDa protein has never been discussed in the literature about molluscan nacre and therefore we decided to further characterize this protein.

Ion exchange chromatography was used as a first purification step. The proteins did not bind to an anion exchanger but cation exchange chromatography was successful. The proteins were bound to CM Sepharose at pH 5 and eluted at different salt concentrations (Figs. 2C and 2D). The pooled fractions shown in Fig. 2D were used for sequencing. This first sequence analysis showed that the 17 kDa protein was new and was named perlucin. Sequence analysis also showed that these perlucin fractions contained a small amount of another unknown protein with an approximate molecular weight of 13 kDa which was called perlustrin. These two proteins were separated from each other and a few remaining contaminants by reversed phase HPLC using a short C4 column (Fig. 3).

					I							G							R											
PL	1	G	C	P	L	G	F	H	Q	N	R	R	S	C	Y	W	F	S	T	I	K	S	S	F	A	E	A	A	G	Y	C	R	Y
ASR	152	C	C	P	V	N	W	V	E	H	E	R	S	C	Y	W	F	S	R	S	G	K	A	W	A	D	A	D	N	Y	C	R	L
LIT	35	S	C	P	E	G	T	N	A	Y	R	S	Y	C	Y	Y	F	N	E	D	R	E	T	W	V	D	A	D	L	Y	C	Q	N
OC	4	G	C	G	P	G	W	V	P	T	P	G	G	C	L	G	F	F	S	R	E	L	S	W	S	R	A	E	S	F	C	R	R
						5					10					15					20					25					30		

FIG. 4. Alignment of the perlucin (PLC) N-terminal sequence to some other C-type lectin domain proteins. ASR, asialoglycoprotein receptor (23). This was the most similar sequence identified by FASTA. LIT, lithostathine (human pancreatic stone protein; 24) and OC, the eggshell protein ovocleidin 17 (21). These 2 proteins were selected because they occur in calcium carbonate biominerals. Amino acids conserved in at least 2 sequences including perlucin are shaded. Positions 4, 11, and 20 of perlucin showed two different amino acids in sequence analysis.

PLS	1	L S C A S C E N A A C P A I G L P - C K - P S E Y V Y T - P C G C X P Q
LU-A	156	L M - A D C Q H Q S C P A - - L P Y C V A P S P N V - T V P C P I G K S

FIG. 5. Alignment of the N-terminal perlustrin sequence with lustrin A. PLS, perlustrin, LU-A, lustrin A (14). The sequence of lustrin A shown is part of the cysteine rich repeat C2. Identical amino acids are shaded.

Sequence of the N-Terminus of Perlucin and Perlustrin and Comparison to Other Proteins

N-terminal amino acid sequence analysis of unmodified and of pyridylethylated perlucin identified the first 32 amino acids of this protein. Comparison of the sequence to known protein sequences showed that it was new. The most similar sequences with up to 45% identical amino acids including three conserved cysteines were those of various C-type lectin domains (Fig. 4). This is a heterogeneous group of proteins with diverse functions (18) which interestingly also encompasses two other proteins isolated from calcium carbonate-containing structures, the pancreatic stone protein lithostathine, which seems to act as an inhibitor of calcium carbonate crystallization in the pancreatic fluid but induces stone formation after proteolytic processing in pancreatits (19) and the avian eggshell protein ovocleidin 17 (20, 21). This indicates that this group of proteins may perform an important, but at present unknown function in biomineralization processes involving calcium carbonate. Two different amino acids were found in cycles 4, 11 and 20 indicating that multiple forms of perlucin exist. N-terminal sequence analysis of perlustrin also yielded more than 30 amino acids. However, the results of database searches were less unequivocal than with perlucin. Among the most similar sequences was a sequence from the nacre matrix protein lustrin A (Fig. 5), a long (1,428 amino acids) multi-domain protein with unknown function (14).

Perlucin Nucleates Calcium Carbonate Crystals

The effect of perlucin on the rate of precipitation of $CaCO_3$ was determined by recording the decrease of pH in a saturated calcium carbonate solution. The initial pH, which depends on the calcium carbonate concentration, was chosen to be 8.7, where calcium carbonate precipitates at room temperature in less than 5 min. Figure 6 shows a series of precipitation experiments with and without perlucin. When the precipitation experiments were done without protein, the time course could be divided into the following steps. First, when $CaCl_2$ is added to $NaHCO_3$ to form the saturated solution, the pH drops suddenly. The cause of this sudden change is not understood but might be due to the formation of a complex between the ionic species which is different from nucleation. Second, there is a slight increase in the pH followed by a relatively stable period for a few tens of seconds. Third, nucleation and precipitation occurs. With perlucin in the solution the sudden drop in pH was immediately followed or even accompanied by nucleation and precipitation of crystals without any lag phase. This is shown in greater detail in Fig. 6B, where we took the first 100 seconds of the experiments and averaged the data from Fig. 6A. As the slope of the precipitation of calcium carbonate with perlucin is just slightly steeper than the precipitation slope of the control measurements we assume that the effect of perlucin is stronger in the nucleation regime than in the promotion of crystal growth. But it can be clearly stated that there is no inhibition of crystal growth by perlucin as was observed with pancreatic stone protein (22). The crystals which were formed in the presence of perlucin and a hydrophobic surface are shown in Fig. 7. There seemed to be a dendritic growth of crystals which was totally absent in

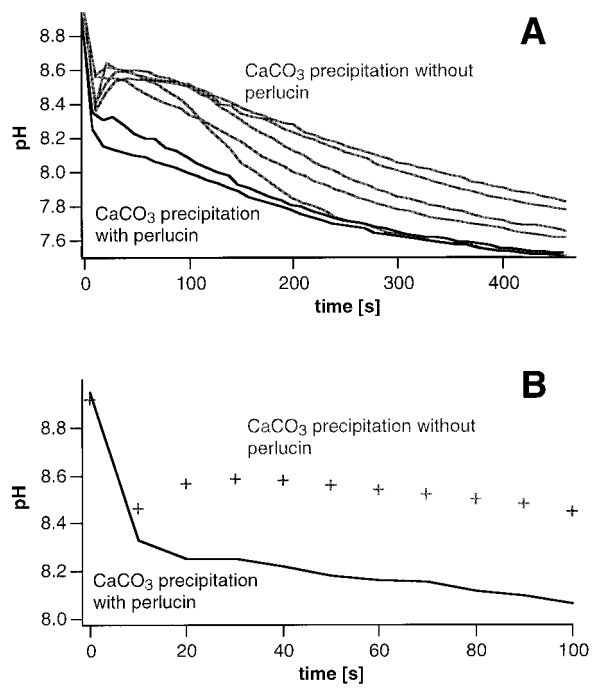

FIG. 6. Recordings of $CaCO_3$ precipitation in a saturated solution. (A) Effect of perlucin on the precipitation of $CaCO_3$. The pH of the solution was recorded as a function of time. When perlucin was present in the solution (black lines), the pH (carbonate concentration) decreased fast without any lag time. This indicates the nucleation and growth of $CaCO_3$ solids. In pure $CaCO_3$ solution (gray lines) nucleation and growth of $CaCO_3$ solids occurred after several minutes. (B) Averages of the data in A for the first 100 s of the pH measurements. After the first sudden drop in pH which occurs in both solutions the pH in the solution with perlucin (line) decreased slowly, whereas the pH in the solution without perlucin (dots) increased first and then remained fairly constant.

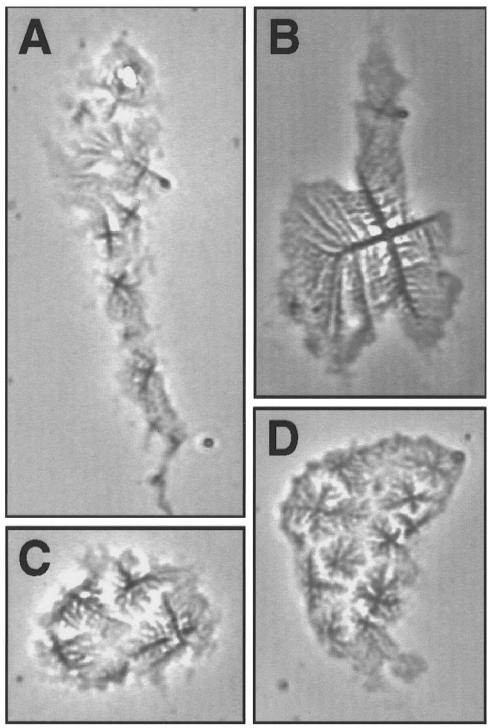

FIG. 7. Light microscopic images of crystals grown in supersaturated calcium carbonate solution in the presence of perlucin. (A–D) Crystals formed in the presence of 0.1 mg/ml perlucin on a cover glass surface. In control solutions the formation of crystals was reduced (not shown).

the control measurements. These results indicate that perlucin may nucleate and bind calcium carbonate crystals and may serve to connect the chitin layer and the aragonite layer.

ACKNOWLEDGMENTS

We very much thank Professor E. Sackmann for fruitful discussions and his kind support. We very much thank Fred Glasbrenner from Australian Abalone Exports for sending us the fresh samples of abalone shells. This work was supported by the Deutsche Forschungsgemeinschaft (I.M.W., M.F.).

REFERENCES

1. Weiner, S., and Addadi, L. (1997) *J. Mater. Chem.* **7,** 689–702.
2. Fritz, M., and Morse, D. E. (1998) *Curr. Opin. Coll. Surf. Sci.* **3,** 55–62.
3. Nakahara, H. (1983) *in* Calcification of Gastropode Nacre (Westbroeck, P., and De Jong, E. W., Eds.), pp. 225–230, Reidel, Dordrecht, Netherlands.
4. Nakahara, H. (1979) *Venus* **38,** 205–211.
5. Weiner, S., Traub, W., and Lowenstamm, H. A. (1983) *in* Organic Matrix in Calcified Exoskeletons (Westbroeck, P., and De Jong, E. W., Eds.), pp. 205–224, Reidel, Dordrecht, Netherlands.
6. Fritz, M., Belcher, A. M., Radmacher, M., Walters, D. A., Hansma, P. K., Stucky, G. D., Morse, D. E., and Mann, S. (1994) *Nature* **371,** 49–51.
7. Schäffer, T. E., Ionescu-Zanetti, C., Proksch, R., Fritz, M., Walters, D. A., Almquist, N., Zaremba, C. M., Belcher, A. M., Smith, B. L., Stucky, G. D., Morse, D. E., and Hansma, P. K. (1997) *Chem. Mat.* **9,** 1731–1740.
8. Currey, J. D. (1980) *in* Mechanical Properties of Mollusc Shell (Vincent, J. F. V., and Currey, J. D., Eds.), pp. 75–97, Cambridge Univ. Press, Cambridge.
9. Cariolou, M. A., and Morse, D. E. (1988) *J. Comp. Physiol. B* **157,** 717–729.
10. Falini, G., Albeck, S., Weiner, S., and Addadi, L. (1996) *Science* **271,** 67–69.
11. Belcher, A. M., Wu, X. H., Christensen, R. J., Hansma, P. K., Stucky, G. D., and Morse, D. E. (1996) *Nature* **381,** 56–58.
12. Walters, D. A., Smith, B. L., Belcher, A. M., Paloczi, G. T., Stucky, G. D., Morse, D. E., and Hansma, P. K. (1997) *Biophys. J.* **72,** 1425–1433.
13. Morse, D. E., Cariolou, M. A., Stucky, G. D., Zaremba, C. M., and Hansma, P. K. (1993) *Mat. Res. Soc. Symp. Proc.* **292,** 59–67.
14. Shen, X., Belcher, A. M., Hansma, P. K., Stucky, G. D., and Morse, D. E. (1997) *J. Biol. Chem.* **272,** 32472–32481.
15. Wheeler, A. P., George, J. W., and Evans, C. A. (1981) *Science* **212,** 1397–1398.
16. Hillner, P. E., Gratz, A. J., Manne, S., and Hansma, P. K. (1992) *Geology* **20,** 359–362.
17. Wada, K. (1972) *Biomineralization* **6,** 141–159.
18. Drickamer, K. (1999) *Curr. Opin. Struct. Biol.* **9,** 585–590.
19. DeCaro, A., Multigner, L., Dagorn, J.-C., and Sarles, H. (1988) *Biochimie* **70,** 1209–1214.
20. Hincke, M. T., Tsang, C. P. W., Courtney, M., Hill, V., and Narbaitz, R. (1995) *Calcif. Tissue Int.* **56,** 578–583.
21. Mann, K., and Siedler, F. (1999) *Biochem. Mol. Biol. Int.* **47,** 997–1007.
22. Multigner, L., DeCaro, A., Lombardo, D., Campese, D., and Sarles, H. (1983) *Biochem. Biophys. Res. Commun.* **110,** 69–74.
23. Spiess, M., Schwartz, A. L., and Lodish, H. F. (1985) *J. Biol. Chem.* **260,** 1979–1982.
24. Moriizumi, S., Watanabe, T., Unno, M., Nakagawara, K. I., Suzuki, Y., Miyashita, H., Yonekura, H., and Okamoto, H. (1994) *Biochim. Biophys. Acta* **1217,** 199–202.